Journal of Thermal Analysis and Calorimetry, Vol. 79 (2005) 313–317

THERMAL DECOMPOSITION OF 5-AMINO-2-THIOL-1,3,4-THIADIAZOLE (*HATT*) Cu(II) AND Zn(II) COMPLEXES

J. C. D'Ars de Figueiredo Jr.[1*], *V. M. De Bellis*[1], *Maria Irene Yoshida*[1], *Vanessa Freitas Cunha Lins*[2] *and L. A. Cruz Souza*[3]

[1]Departamento de Química, ICEx – Universidade Federal de Minas Gerais, 31.270-901 Belo Horizonte, MG, Brazil
[2]Departamento de Engenharia Química, Universidade Federal de Minas Gerais, Brazil
[3]LACICOR, CECOR, Departamento de Artes Plásticas, Escola de Belas Artes, Universidade Federal de Minas Gerais, Brazil

Complexes of Cu(II) and Zn(II) with 5-amino-2-thiol-1,3,4-thiadiazole (*HATT* – $C_2H_3N_3S_2$) can be obtained by the reaction of *HATT* with copper alloy corrosion products, which makes these complexes useful in the industrial field and in the conservation of bronze cultural heritage. This paper describes the study of the thermal decomposition of these complexes. TG/DTG, DTA, vibrational spectroscopy, X-ray diffraction and elemental analysis have been performed. Gaseous products (CO_2, SO_2, NO_2 and H_2O) were evolved during the thermal decompositions. The final residues were CuO and ZnO.

Keywords: *copper alloy corrosion, HATT, thermal analysis*

Introduction

The ligand $C_2H_3N_3S_2$ (5-amino-2-thiol-1,3,4-thiadiazole, *HATT*) is a tautomeric compound (Fig. 1) used in the protection of metal corrosion, which is the subject of several papers [1–5]. Some of them are used in the protection of stainless steel parts of paper producing machines working with pulp-brightening [2] and in the conservation of bronze cultural heritage [3, 4].

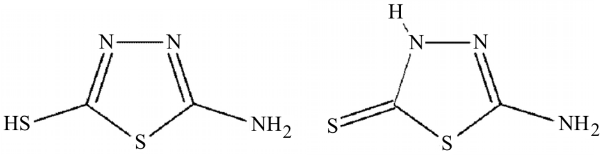

Fig. 1 Tautomeric structures of 5-amino-2-thiol-1,3,4-thiadiazole; left – thiol- and right – thione forms

When corroded metal pieces are immersed in the solution of this compound, it reacts with the products of corrosion and results metal complexes. In case of copper and copper alloys, the major corrosion products are basic copper(II) salts, e.g. basic copper chloride ($CuCl_2 \cdot 3Cu(OH)_2$ – paratacamite) and basic copper carbonate ($CuCO_3 \cdot Cu(OH)_2$ – malachite). The formed metal complex is $[Cu(C_2H_2N_3S_2)_2 \cdot H_2O]$. Depending on the constitution of alloy (which may contain Zn, Sn and Pb) and atmosphere (which may contain CO_2, SO_2 and chlorides), other products may be obtained [6]. In our research work, the thermal decomposition of two complexes, $[Cu(C_2H_2N_3S_2)_2 \cdot H_2O]$ and $[Zn(C_2H_2N_3S_2)_2 \cdot H_2O]$ have been studied. Simultaneous TG/DTG and DTA curves were recorded. Intermediate products were characterized using infrared spectroscopy (IR), X-ray diffraction (XRD) and elemental analysis.

Experimental

Preparation of compounds

Ligand

HATT was synthesized according to [7]. 200 mg of *HATT* was dissolved in 30 mL of 1:1 water–ethanol solution and then was neutralized with 0.1 mol L^{-1} ammonia solution until pH=7.44 was reached. This neutralization was necessary to provide the presence of the thiolate ion in solution ($C_2H_2N_3S_2^-$ – *ATT*) [8]. The product of neutralization was $NH_4C_2H_2N_3S_2$ (NH_4ATT).

Basic copper(II) salts

Basic copper(II) chloride ($CuCl_2 \cdot 3Cu(OH)_2$) and basic copper(II) carbonate ($CuCO_3 \cdot Cu(OH)_2$) was synthesized as it have been reported in [9, 10].

---

[*] Author for correspondence: jcdfj@dedalus.lcc.ufmg.br

1388–6150/$20.00

Akadémiai Kiadó, Budapest, Hungary
Springer, Dordrecht, The Netherlands

$[Cu(C_2H_2N_3S_2)_2{\cdot}H_2O]$

214 mg of $CuCl_2{\cdot}3Cu(OH)_2$ was dissolved in 30 mL of distilled water at 60°C, and then NH_4ATT solution was added. After 1 h of agitation, the obtained solid was filtered, washed with hot water and ethanol and dried at reduced pressure. The same procedure was carried out with 221 mg of $CuCO_3{\cdot}Cu(OH)_2$, to obtain the same complex.

$[Zn(C_2H_2N_3S_2)_2{\cdot}H_2O]$

201 mg of $ZnSO_4{\cdot}7H_2O$ was dissolved in 20 mL of distilled water. Then NH_4ATT was added to this solution. After 30 min of agitation, the obtained solid was filtered, washed with hot water and ethanol and dried at reduced pressure.

Analysis

The thermal decomposition of the complexes was investigated using Netzsch STA 409EP thermobalance. TG/DTG and DTA curves were recorded simultaneously. The analysis was done in air atmosphere with a flow rate of 100 mL min^{-1} and at a heating rate of 10°C min^{-1}. Infrared spectra have been recorded with a Perkin Elmer Spectrum GTX – FTIR unit in the range of 4000–400 cm^{-1}, with 4 cm^{-1} resolution. X-ray diffractograms were collected using a Rigaku Geigerflex 2037 diffractometer. Elemental analysis (CHN) was made using a CHN Perkin Elmer 2400 apparatus and the metal content was determined by AAS method using Hitachi Z-8200 Atom Absorption Spectrometer. Melting points were determined using a Mettler FP-5 apparatus.

Results and discussion

According to the X-ray diffraction patterns, the complexes precipitated in their amorphous forms, as it could be observed (curves are not presented). The expected composition for the complexes were confirmed by elemental analysis. The results are given in Table 1.

The representative TG/DTG and DTA curves of the thermal decomposition of $[Cu(C_2H_2N_3S_2)_2{\cdot}H_2O]$ complex showed many mass loss steps, which can be classified into four temperature ranges: 35–150, 150–350, 350–600 and 600–950°C. Curves are given in Fig. 2.

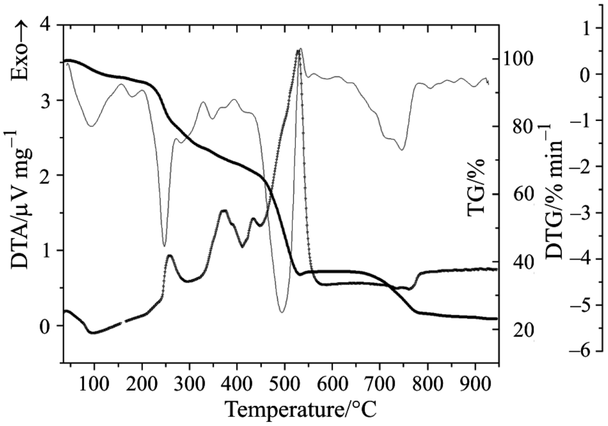

Fig. 2 TG/DTG and DTA curves of the thermal decomposition of $[Cu(C_2H_2N_3S_2)_2{\cdot}H_2O]$ complex

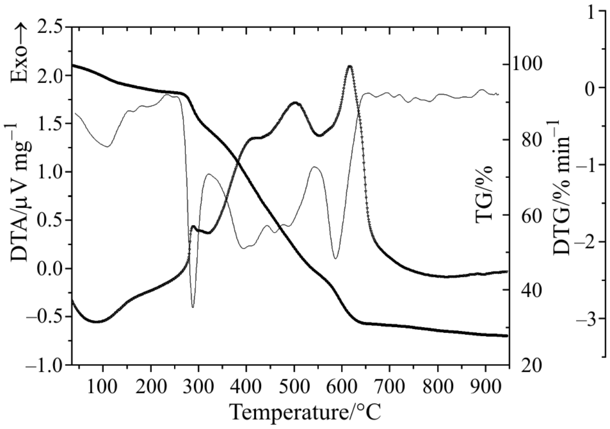

Fig. 3 TG/DTG and DTA curves of the thermal decomposition of $[Zn(C_2H_2N_3S_2)_2{\cdot}H_2O]$ complex

The TG/DTG and DTA curves of the thermal decomposition of $[Zn(C_2H_2N_3S_2)_2{\cdot}H_2O]$ complex showed several mass loss steps which can be ordered into three different temperature ranges: 35–150, 150–325 and 325–950°C (Fig. 3).

The first mass loss appeared between 35–150°C for both complexes, wich corresponds to the loss of 1 molecule of water. The mass loss was 4.9% for

Table 1 Compositions of complexes

Complex	*M*/%		C/%		H/%		N/%		Melting point
	calc.	found	calc.	found	calc.	found	calc.	found	
$[Cu(C_2H_2N_3S_2)_2{\cdot}H_2O]$	19.4	20.2	13.9	13.8	1.7	1.3	24.3	23.2	Decomposition without fusion
$[Zn(C_2H_2N_3S_2)_2{\cdot}H_2O]$	18.8	19.8	13.8	13.5	1.7	1.7	24.2	22.0	Decomposition without fusion

$[Cu(C_2H_2N_3S_2)_2{\cdot}H_2O]$ and 5.4% for $[Zn(C_2H_2N_3S_2)_2{\cdot}H_2O]$. They were accompanied by an endothermic event, as they are shown in the DTA curve. The equations for these losses are represented below:

$$[Cu(C_2H_2N_3S_2)_2{\cdot}H_2O]\rightarrow[Cu(C_2H_2N_3S_2)_2]+H_2O \quad (1)$$

$$[Zn(C_2H_2N_3S_2)_2{\cdot}H_2O]\rightarrow[Zn(C_2H_2N_3S_2)_2]+H_2O \quad (2)$$

The second temperature range was 150–350°C for $[Cu(C_2H_2N_3S_2)_2{\cdot}H_2O]$ complex and 150–325°C for $[Zn(C_2H_2N_3S_2)_2{\cdot}H_2O]$. The X-ray diffractograms for the $[Cu(C_2H_2N_3S_2)_2{\cdot}H_2O]$ product showed a few small peaks, but an amorphous character was predominant. In case of $[Zn(C_2H_2N_3S_2)_2{\cdot}H_2O]$ the X-ray patterns still showed an amorphous compound. C, H and N elemental analysis of products in these temperature ranges are given in Table 2.

The most reliable change of these compounds is observed in their vibrational spectra. The vanishing of the νC=N band at 1540 cm^{-1} indicating the elimination of a N atom from the ring. A band attributed to δN–H, originating from the amino group [11], at ≅1600 cm^{-1}, is present in the spectra of these products, which confirms that the N atom originates from the ring. The comparison of these spectra (complexes and products in the temperature ranges of 150–350 and 150–325°C) is given in Fig. 4.

The observed mass loss in these ranges was of 21.0% for $[Cu(C_2H_2N_3S_2)_2{\cdot}H_2O]$ and 12.4% for $[Zn(C_2H_2N_3S_2)_2{\cdot}H_2O]$. The DTA curve showed exotherm peaks in this range, indicating that oxidation takes place. The results of elemental analysis, vibrational spectroscopy and thermal analysis led us to establish the following equations for the decompositions concerning to the second temperature ranges:

$$[Cu(C_2H_3N_3S_2)_2]+5O_2\rightarrow$$
$$\rightarrow CuC_3H_2N_4S_3+CO_2+2H_2O+2NO_2+SO_2 \quad (3)$$

$$[Zn(C_2H_3N_3S_2)_2]+4.75O_2\rightarrow$$
$$\rightarrow ZnC_3HN_5OS_3+CO_2+2.5H_2O+NO_2+SO_2 \quad (4)$$

The X-ray diffractogram of the product of Cu(II) complex in the third temperature range (350–600°C) (Fig. 5) showed defined peaks which can be attributed to the mixture of $CuSO_4$ and CuO. Bands of sulphate [11] were observed in the infrared spectra of this product at 1152, 1110 (asymmetric stretching), 1072 (symmetric stretching), 879 and 852 cm^{-1} (bending), respectively.

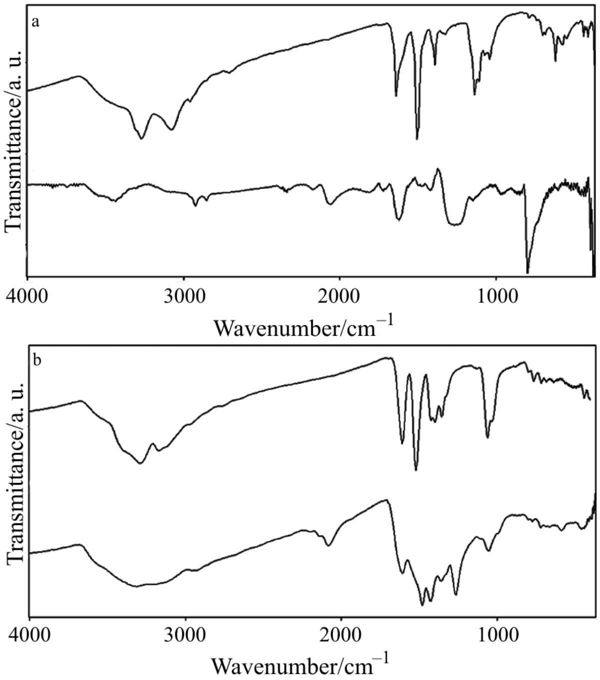

Fig. 4 Comparison of vibrational spectra of a – $[Cu(C_2H_2N_3S_2)_2{\cdot}H_2O]$ and b – $[Zn(C_2H_2N_3S_2)_2{\cdot}H_2O]$ complexes to the spectra of the products of the thermal decomposition between a – 150–350°C and b – 150–325°C, respectively

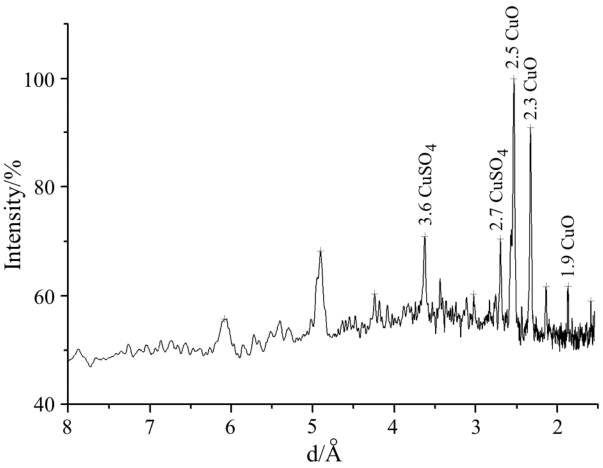

Fig. 5 X-ray diffractogram of the products obtained by the thermal decomposition of $[Cu(C_2H_3N_3S_2)_2{\cdot}H_2O]$ in the range of 350–600°C. Peaks are attributed to $CuSO_4$ and CuO

Table 2 C, H and N elemental analysis of formed products in two temperature ranges

End-products	Temperature range/°C	C/%		H/%		N/%	
		calc.	found	calc.	found	calc.	found
$CuC_3H_2N_4S_3$	150–350	14.2	13.8	0.8	0.9	22.1	24.8
$ZnC_3HN_5OS_3$	150–325	12.7	14.7	0.4	0.3	24.6	25.4

Table 3 Proposed decomposition steps and the respective mass losses of $[Cu(C_2H_3N_3S_2)_2 \cdot H_2O]$

Equations	Temperature range/°C	Δ*m*/%	
		calc.	exp.
$[Cu(C_2H_3N_3S_2)_2 \cdot H_2O] \rightarrow [Cu(C_2H_3N_3S_2)_2]+H_2O$	35–175	5.2	4.9
$[Cu(C_2H_3N_3S_2)_2]+5O_2 \rightarrow [CuC_3H_2N_4S_3]+CO_2+2H_2O+2NO_2+SO_2$	175–350	22.0	21.0
$2[CuC_3H_2N_4S_3]+22.5O_2 \rightarrow CuSO_4 \cdot CuO+5SO_2+2H_2O+8NO_2+6CO_2$	350–600	38.8	37.2
$CuSO_4 \cdot CuO \rightarrow 2CuO+SO_3$	600–950	13.9	13.7

Table 4 Proposed decomposition steps and the respective mass losses of $[Zn(C_2H_3N_3S_2)_2 \cdot H_2O]$

Equations	Temperature range/°C	Δ*m*/%	
		calc.	exp.
$[Zn(C_2H_3N_3S_2)_2 \cdot H_2O] \rightarrow [Zn(C_2H_3N_3S_2)_2]+H_2O$	35–175	5.2	5.4
$[Zn(C_2H_3N_3S_2)_2]+4.75O_2 \rightarrow [ZnC_3HN_5S_3]+CO_2+2.5H_2O+NO_2+SO_2$	175–325	12.9	12.4
$[ZnC_3HN_5S_3]+11.25O_2 \rightarrow ZnO+3SO_2+0.5H_2O+5NO_2+3CO_2$	325–950	53.8	54.4

The diffractogram of the product of the thermal decomposition of Zn(II) complex in the third temperature range (325–950°C) showed defined peaks which were attributed to the presence of ZnO (Fig. 6).

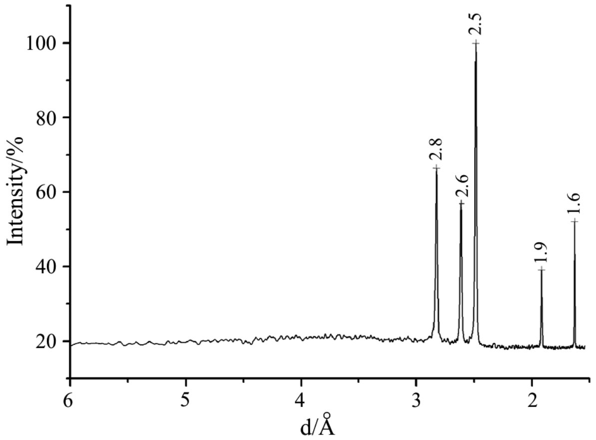

Fig. 6 Diffractogram of the end-products of the thermal decomposition of $[Zn(C_2H_3N_3S_2)_2 \cdot H_2O]$ obtained in the range of 325–950°C. Peaks attributed to ZnO

The mass loss for the Cu(II) complex was 37.2 and 54.4% for the Zn(II) complex. The DTA curves show exotherm peaks in these ranges, which confirm the oxidation reactions. According to the results of X-ray diffraction and thermal analysis, the following equations can be established:

$$2CuC_3H_2N_4S_3+22.5O_2 \rightarrow \rightarrow CuSO_4 \cdot CuO+5SO_2+2H_2O+8NO_2+6CO_2 \quad (5)$$

$$ZnC_3HN_5OS_3+11.25O_2 \rightarrow \rightarrow ZnO+3SO_2+0.5H_2O+5NO_2+3CO_2 \quad (6)$$

The diffractogram of the product of the fourth temperature range of decomposition of $[Cu(C_2H_2N_3S_2)_2 \cdot H_2O]$ showed the presence of CuO. The recorded mass loss is 13.7%, while the supposed decomposition path is the following:

$$CuSO_4 \cdot CuO \rightarrow 2CuO+SO_3 \quad (7)$$

All thermal decomposition steps proposed for the two complexes are shown in Tables 3 and 4.

Conclusions

The thermal decomposition of $[Cu(C_2H_3N_3S_2)_2 \cdot H_2O]$ and $[Zn(C_2H_3N_3S_2)_2 \cdot H_2O]$ complexes in air exhibits mainly oxidation reactions which was proven by DTA, generating CO_2, SO_2, NO_2 and H_2O gaseous products similarly to [12]. The first mass loss for both complexes, corresponds the loss of 1 molecule of water. During the next mass losses gaseous compounds (see above) are generated. The final residues are CuO and ZnO. The equations representing the thermal decomposition in the whole temperature range (35–950°C) and suggest the formation of different intermediate products, which were supported by infrared spectroscopy, elemental analysis (CHN) and X-ray diffraction (XRD).

Acknowledgements

This work was supported by FAPEMIG.

References

1 F. Zucchi, ACH – Models in Chemistry, 132 (1995) 579.

2 K. S. K. Danadurai and S. Rajeswari, Bull. Electrochem., 13 (1997) 99.

3 M. C. Ganorkar, V. P. Rao, P. Gayathri and T. A. S. Rao, Stud. Conservation, 33 (1988) 97.

4 R. Faltermeier, Stud. Conservation, 44 (1998) 121.

5 L. Ying, F. Haitao, Z. Yifan and W. Wuji, J. Mater. Sci., 38 (2003) 407.

6 D. A. Scott, Copper and bronze in art, The Getty Conservation Institute, Los Angeles 2002.

7 J. Sandstrom, Acta Chem. Scand., 15 (1961) 1300.

8 E. E. Chufán, J. C. Pedregosa and J. Borrás, Vibr. Spectrosc., 15 (1997) 191.

9 A. M. Pollard, R. G. Thomas and P. A. Williams, Min. Mag., 53 (1989) 557.

10 H. Tanaka and M. J. Yamane, J. Thermal Anal., 38 (1992) 629.

11 L. J. Bellamy, Infrared Spectra of Complex Molecules, Wiley and Sons, New York 1954.

12 M. Badea, R. Olar, D. Marinescu, M. Brezeanu, C. Cälina-Soradi and E. Segal, Thermochim. Acta, 279 (1996) 183.